# Ambient-RF-Energy-Harvesting Sensor Device with Capacitor-Leakage-Aware Duty Cycle Control

Ryo Shigeta, *Member, IEEE,* Tatsuya Sasaki, Duong Minh Quan, Yoshihiro Kawahara, *Member, IEEE,* Rushi J. Vyas, *Student Member, IEEE,* Manos M. Tentzeris, *Fellow, IEEE,* and Tohru Asami, *Member, IEEE*

***Abstract*—In this paper, we present a software control method that maximizes the sensing rate of wireless sensor networks (WSNs) that are solely powered by ambient RF power. Unlike all other energy-harvesting WSN systems, RF-powered systems present new challenges for energy management. A WSN node repeatedly charges and discharges at short intervals, depending on the energy intake. Typically in energy-harvesting systems, a capacitor is used for an energy storage because of its efficient charge and discharge performance and infinite recharge cycles. When the charging time is too short, a node is more likely to experience an energy shortage. On the contrary, if it is too long, more energy is lost because of leakage in the capacitor. In this paper, we introduce an adaptive duty cycle control scheme optimized for RF energy harvesting. This method maximizes the sensing rate by taking into account the leakage problem, a factor that has never been previously studied in this context. Our control scheme improves the efficiency by aggregate evaluation of operation reliability and leakage reduction.**

***Index Terms*—Ambient RF Energy Harvesting, Digital TV, Capacitor, Duty Cycle Control, Wireless Sensor Networks**

## I. Introduction

Energy harvesting devices such as solar panels, piezoelectric devices, thermocouples, and RF energy scavengers are attracting a great deal of attention, especially in applications related to low-power Wireless Sensor Networks (WSNs) [1], [2], [3]. Energy harvesting can dramatically extend the operating lifetime of nodes in wireless sensor networks. Furthermore, this technology enables a battery-less operation and reduces the operation cost of WSNs, which is mainly due to battery replacement, thus making it very important for a sustainable "near-perpetual" WSN operability. Thus, energy harvesting is important for the sustainable operations of a WSNs. In this study, we focus on RF energy harvesting, which can produce only a small amount of energy; however, it is more stable than solar and wind power. On another front, RF energy harvesting has specific characteristics not found in other energy sources. For instance, because we rely on "ambient" RF signals, which are originally intended for other communication and broadcast systems, the amount of harvested energy comprises both a long-term fluctuation due to radio tower service schedules and human activity patterns, and short-term variability due to fading and noise. Therefore, in this paper we introduce a novel energy management method that is robust against both these issues. In low-power WSN systems, the sensor nodes attempt to save energy by being in "sleep" mode almost throughout the entire time and periodically switching to the active mode only when a sensing task is assigned. The ratio of the active time to total cycle time is called a duty cycle. A typical ultralow-power microcontroller operates in the following three modes: active, sleep, and off. Unlike the off-mode, the sleep mode consumes a few dozen nA; however, the microcontroller can maintain the status of the register and resume the task with a minimum time and power overhead. The adaptive duty cycle management plays an important role in balancing the energy intake and expenditure. When a sensor node is set in a duty cycle that is too high compared to harvested energy, the sensor node consumes the stored energy and finally turns off because of energy shortage. After the sensor node is off, it consumes 5 times more energy for turning into active mode compared to wake up from sleep to active. Therefore, a duty cycle control method should be designed to avoid the energy shortage risk, which we call a "dead" risk. On the other hand, a lower duty cycle is not desirable because of the leaky characteristics of energy storages. In this study, we used capacitors for energy storage because of their charge and discharge efficiency. Capacitors are better than batteries in this respect and have no limitation on the number of recharge/discharge cycles. However, capacitors yield more energy leakage than batteries, for example, the leakage of a NiMH battery, which is the most leaky battery, is 30% per month, while the leakage of a super capacitor is 5.9% per day [4]. Therefore, we had to deal with the capacitor leakage problem as it results in a relatively large amount of energy loss in comparison to scavenged amount of energy obtained from a harvester. The contributions of this study are summarized as follows; (1) implementation of low-cost RF energy harvesting sensor nodes using inkjet printing; (2) Introduction of the optimal stored energy level calculation by the aggregate evaluation of capacitor leakage and the energy shortage risk; (3) adaptive optimal operation point tracking, taking into account harvested energy variability; and (4) evaluation of the duty cycle control algorithm via simulation with measured TV radio wave data. By using the proposed method, we achieve a 5.34% leakage reduction compared with a method that does not involve operation point tracking. Our proposed method can reduce the capacitor leakage by the determination of the optimal capacitor stored energy. In addition, the optimal

R. Shigeta, T. Sasaki, D. M. Quan, Y. Kawahara and A. Tohru are with the Graduate School of Information Science and Technology, The University of Tokyo, 7-3-1, Hongo, Bunkyo-ku, Tokyo, Japan. E-mail: (see http://akg.t.u-tokyo.ac.jp/).

Y. Kawahara, R. J. Vyas and M. M. Tentzeris are with the School of Electrical and Computer Engineering Georgia Institute of Technology, Atlanta, GA 30332-250, USA.

An earlier version of this paper was presented at the IEEE SENSORS 2012 Conference and was published in its Proceedings.

Manuscript revised on May 22, 2013.

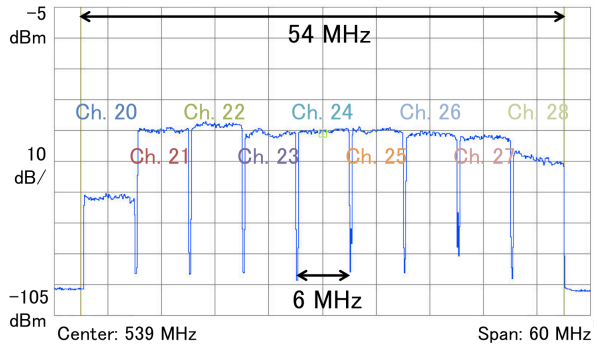


Fig. 1. Spectrum of ISDB-T digital TV signal.

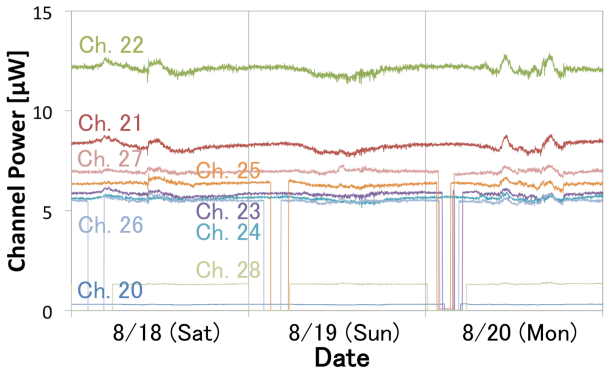


Fig. 2. Channel power of digital TV broadcasting signal for 3 days. Some channels stop transmitting in midnight, thus accentuating channel power time-variability

stored energy adjustment is adaptively performed with regard to both short-term and long-term transitions of the harvested energy. We can achieve an optimally efficient energy usage and a maximized sampling/sending rate applying the energy management strategies introduced in this paper.

## II. Related Work

Ambient RF energy harvesting has been discussed in several feasibility studies and prototype implementations. The target frequencies of the ambient RF energy harvesting are mainly on 500 MHz, 900 MHz, and 2.45 GHz. For example, Parks et al. successfully performed a sensor node operation using RF energy harvesting from a 500-MHz digital TV broadcasting radio wave. Their sensor node could operate at a distance of 10.4 km from broadcasting tower with a transmission power of 1 MW [5]. In addition, they implemented a sensor node powered by a cellular Base Transceiver Station (BTS) at a distance of 200m from the BTS. Dolgov et al. designed a Maximum Power Point Tracking (MPPT) mechanism for RF energy harvesting, considering the variability in the transmitted power from the BTS's [6]. They considered wireless sensors for cellular tower monitoring that can harvest energy from the side-lobe or reflected RF power and monitor the tower activities [7]. The frequency of 2.45 GHz is widely used for communications such as Wi-Fi and Bluetooth. Olgun et al. developed a technique to continuously drive a temperature and humidity sensor with a LCD using Wi-Fi RF energy

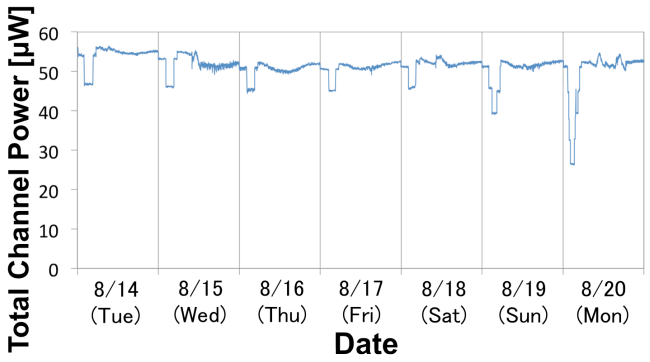


Fig. 3. Total channel power of digital TV broadcasting signal for a week.

harvesting [8]. A compact and efficient rectenna operating at 2.45 GHz was designed by the optimization of patch antennas and a charge pump [9]. On the other hand, 2.45 GHz is commonly used for microwave wireless power transmission [10], using the technologies that are almost the same as those applicable for ambient RF energy harvesting. In this study, we considered a low-cost ambient RF energy harvesting sensor node using a digital TV broadcasting signal. The sensor node should be applicable in structural health monitoring or "rugged" environmental monitoring because these applications do not require sensing at fixed intervals; however, a battery-less and low-cost operation is desirable. As mentioned above, there have been some of studies on the design of a RF energy scavenger using a TV signal. Nishimoto and Vyas designed a RF energy scavenger that could capture the RF power of a TV signal using an inkjet-printed dipole antenna and a charge pump [11], [12]. Vyas, Kawahara and Tentzeris were the first to identify and exploit the multi-channel OFDM nature of TV signals for powering an embedded microcontroller [13]. However, several challenges faced by energy management software remain unsolved. A TV broadcasting signal wave is much more stable than wireless communication signals such as those utilized in cell phones; however, it commonly varies dynamically around midnight because of the scheduled facility maintenance as shown in Figure 2. To address this issue, we develop a capacitor-leakage-aware duty cycle control method for ambient RF energy harvesting. A general software management method for energy harvesting sensor node has already been developed. However, a method particularly focusing on the ambient RF energy harvesting is yet to be developed. We proposed capacitor-leakage-aware duty cycle control method that considers generic energy harvesting sensor nodes [14]. Our method can work more effectively when energy supply from harvester has both long-term and short-term fluctuations, thus being very appropriate for RF energy harvesting.

## III. Variability of Harvested TV Energy

The digital TV broadcast in Japan is performed using the Integrated Service Digital Broadcasting-Terrestrial (ISDB-T) standard. In addition, the ISDB-T standard is used in the Philippines and South America, while the Digital Video Broadcasting-Terrestrial (DVB-T) standard is mainly used in Europe. Both ISDB-T and DVB-T have many common

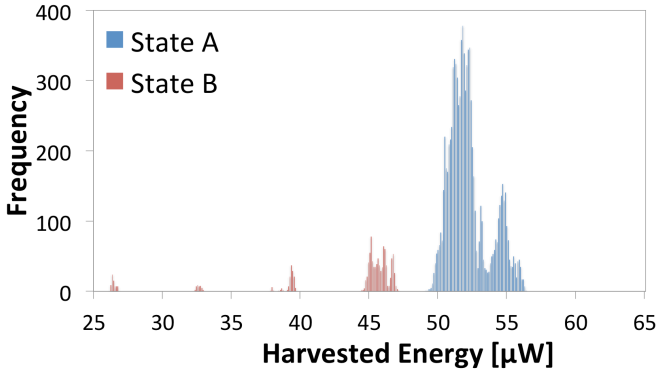


Fig. 4. Histogram of total channel power of TV signal. Some channels are interrupted at midnight, thus total channel power state shifts to State B.

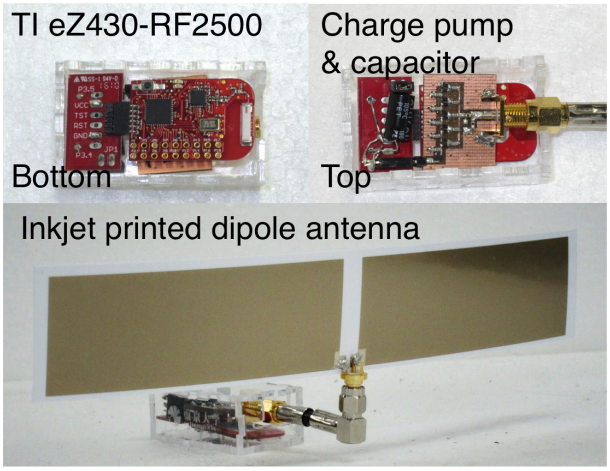


Fig. 5. Prototype of TV radiowave energy harvesting sensor node.

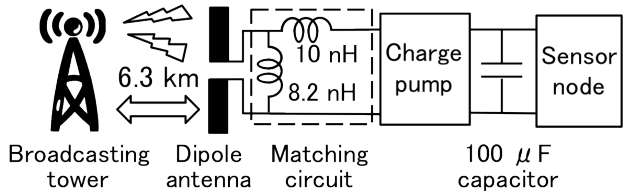


Fig. 6. System overview of RF energy harvesting sensor node.

features, that is, both of them use OFDM modulation, and therefore, they can be considered as almost the same signal for ambient RF energy harvesting. Figure 1 show the spectrum of the ISDB-T broadcasting signal used in Tokyo. There are nine channels (Ch. 20 to 28) each with a bandwidth of 6 MHz at frequencies ranging 512 MHz to 566 MHz. Ch. 21 to 27 are transmitted from the Tokyo tower with 48 kW (Equivalent Radiated Power: ERP). In this spectrum, Ch. 20 and 28 are comparatively weaker than the other channels because Ch. 20 is transmitted with 5 kW (ERP) and Ch. 28 with 19 kW (ERP). In this case, we plan to continuously operate the sensor node that can measure temperature data at our building that is approximately 6.3 km away from the Tokyo tower. Using following Friis's equation, the received power at the dipole antenna at this position can be estimated as from 30 to 100 $\mu$W [12], [13].

$$P_R = P_T G_T G_R (\frac{\lambda}{4\pi R})^2 \quad (1)$$

An accurate estimation of the received power is quite difficult because the received power is affected by the reflection at the ground and fading; however, several dozen microwatts is required to periodically drive the sensor node. Considering these circumstances, we use digital TV signals as an energy source. Figure 2 shows typical average channel power data of these channels measured in 3 days. These data are measured at 1-min interval. Each channel occupies in total 6 MHz. The channel power is measured using a 5-dBi YAGI UwPA UHF antenna [15] connected to a Tektronix RSA-3308B real-time spectrum analyzer. Although the measurement setup is not the same as our sensor node setup, the objective of this measurement is to measure the relative change in the channel power, thus the absolute value of individual channel power levels does not need to be accurately measured. As can be observed from the measurement result, the total channel power level is divided into two states. This is mainly because some of the channels stop the broadcasting service at midnight for energy saving and/or maintenance purposes. It is quite difficult to predict when and which channel stops sending signal. When all the channels are broadcasting, the total amount of channel power varies because of fading and noise; however, the variation is not abrupt. We defined this "total-channel-power" state as State A. At midnight, some of channels are turned off owing to the broadcasting schedule and maintenance. Ch. 26 and Ch. 28 are stopped almost every midnight; however Ch. 22 and 21 are not stopped all the time and the remaining channels are only stopped from midnight to early morning during weekends. We define this "total-channel-power" state as State B. Figure 3 shows the total power from the TV radio signal consisting of 9 channels for a week including the daily fluctuation, which is given by the broadcasting schedules. However, these signals exhibit a short-term variability. Figure 4 shows a histogram of the channel power that represents the probability distribution function of the supplied energy required for the death risk estimation. When some of the channels are turned off and the transmitted energy decreases, the variability in the harvested energy decreases, and therefore, we should recalculate the optimal stored energy level at this transition. The current variability can be estimated from the average harvested energy, and our proposed method appropriately sets the optimal level in each state. This type of daily transition of the channel power can be observed in the communication signal transmitted from the cellular BTSs [16]. Thus, energy management methods for ambient RF energy harvesting should consider the signal characteristics.

## IV. Design of Sensor Node

To evaluate the performance of our novel energy management approach, we design a prototype of an ambient RF energy harvesting sensor node, as shown in Figure 5, using the scavenged energy from the digital TV broadcasting signals. As shown in Figure 6, this sensor comprises of the following

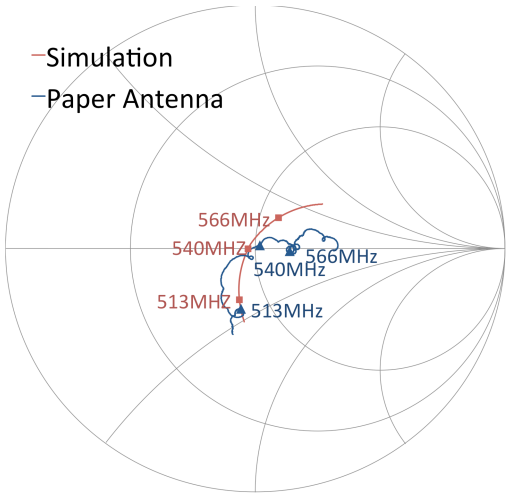


Fig. 7. S11 parameter of inkjet-printed dipole antenna on Smith chart.

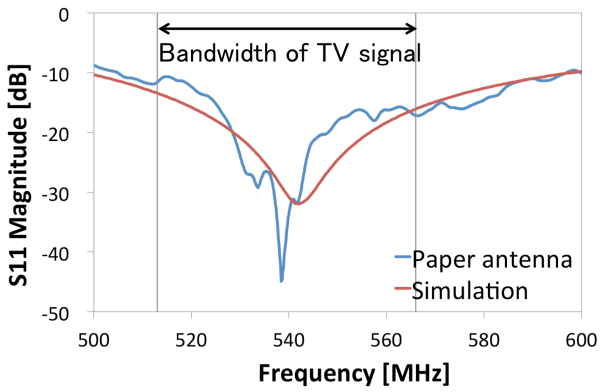


Fig. 8. S11 parameter of inkjet-printed dipole antenna, with magnitudes in dB.

four modules: (1) inkjet-printed dipole antenna, (2) 5-step modified Dickson charge pump with matching circuit, (3) 100-$\mu$F capacitor and (4) a Texas Instruments eZ430 RF-2500 sensor node with temperature sensor [17]. In this section, we discuss the design of these components. Note that the combination of an antenna and a rectifier including charge pump is called "rectenna" and it works as a converter of the RF ambient signal to DC power.

### A. Ink-jet-Printed Dipole Antenna

We use the inkjet printing technology with a conductive silver nano ink manufactured by Mitsubishi Paper Mills Limited [18], to fabricate an antenna at a low cost. The antennas for ambient RF energy harvesting from TV radio wave should have a wide bandwidth to cover spectrum of 54 MHz around the central frequency in order to capture energy from 9 ISDB-T channels that can be observed in Tokyo area. By increasing the width of the element, it is possible to expand the bandwidth of the dipole antenna. We conducted a simulation of the antenna design using Sonnet to determine the optimal width of the antenna elements. In this simulation, we used a 0.35-mm thick PET-film photo paper model, with a relative permittivity of 3.0 and a loss tangent of 2.1%, and 1-$\mu$m thick conductive pattern model. Finally, we achieve the optimal elements size of 104 mm x 36 mm. The thickness of the ink is only 1 micrometers and the conductivity of the silver ink is 7.7 MS/m. The wider pattern contributed to reduction in the antenna resistance. Figure 7 and 8 show the value of the return loss S11 of the printed antenna with good agreement between the simulations and the measurements. The simulated antenna gain value was 1.33 dBi. Although there are some errors, the simulated S11 parameter is roughly fit to the actual S11 at the working bandwidth.

### B. 5-Stages Modified Dickson Charge Pump

A modified Dickson charge pump is often used as a RF/DC converter for the RF energy harvester because it converts RF power to DC and works as a voltage multiplier [19]. On the other hand, some RF energy scavenging systems use a half-wave rectifier or a voltage doubler rectifier, connected to an ultra low-power charge pump IC such as S882-Z manufactured by Seiko Instruments [20]. When the distance from the TV tower is far and the received power is not enough high (lower than -10 dBm approximately), the combination of a rectifier and a charge pump IC works better than the Dickson charge pump. However, if the signal is strong enough, the Dickson charge pump can efficiently supply higher amounts of energy [5]. In our scenario, although the sensor node is placed several kilometers far from the TV tower, the received power is sufficient to enable the Dickson charge pump to operate efficiently and supply the sufficient voltage. Although some of the suppliers have begun to develop ultra low-power charge pump ICs, only a few types of the product are available on the market and they have not been commonly used yet. Considering the mass production of low-cost sensors, the Dickson charge pump is more suitable because it is composed of easily available capacitors and Schottky diodes, that are commonly used for signal detection applications. Obviously, whenever ultralow-power charge pump ICs become common and inexpensive, we should reconsider the design of a RF/DC converter. SMS-7630 [21] manufactured by Skyworks Solutions is often chosen for low-power charge pump circuits owing to its lower threshold voltage [22]. Figure 6 shows our charge pump schematics. We use SMS-7630 for the charge pump except for the final diode that blocks the reverse current from the energy storage due to the very low value of its reverse resistance [21]. Avago HSMS-286C [23] exhibits a higher resistance and is more suitable to use as the final diode instead. If we increase the number of stages in the charge pump, a higher voltage is generated; however the total efficiency decreases, thus making it necessary to choose the minimum number of stages that supplies sufficient voltage to activate the sensor node. In our case, the received power is estimated as several dozens to a hundred microwatts as reported by Nishimoto and Vyas in [11] and [13]. With a 100-$\mu$W input power, a 3-stage charge pump generates 1.8 V, a 4-stage charge pump generates 2.2 V, and a 5-stage charge pump generates 2.7 V on a circuit simulation. Typical sensor nodes turn-on voltages range between 1.8 V - 3.6 V, thus requiring at least four-stage charge

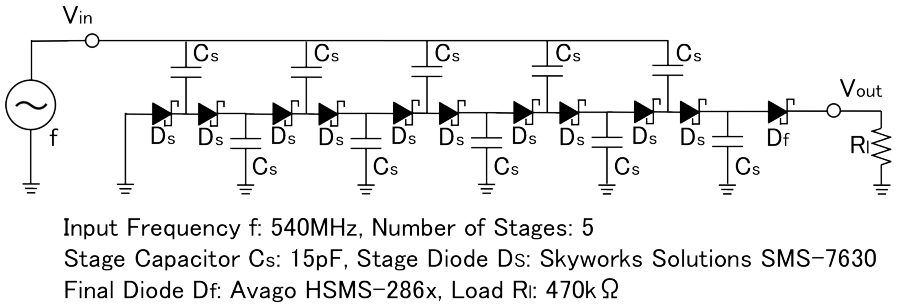


Fig. 9. Schematics of a 5-stage modified Dickson charge pump.

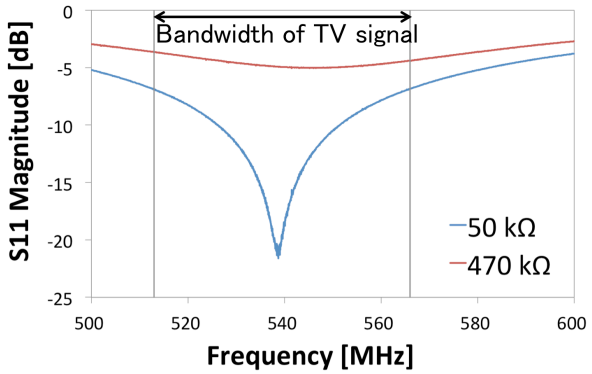


Fig. 10. S11 values for the charge pump in dB.

pumps. For the sake of safety, considering an input power fluctuation, a 5-stage charge pump is suitable for our study. The input resistance of the charge pump was measured using a Rohde & Schwarz ZVL-3 vector network analyzer with -10 dBm input signal. The resistance in the TV signal bandwidth (from 513 MHz to 566 MHz), without connecting a matching circuit, show losses of between 5.88 and 7.58 Ω and capacitive reactance between 34.9 and 41.1 Ω for a 470 kΩ load. In addition, it shows losses of between 8.09 and 10.13 Ω and capacitive reactance between 33.6 and 40.0 Ω for a 50 kΩ load respectively. Note that we utilized 470 kΩ load to simulate the sensor node in sleep-mode, while a load of 50 kΩ maximizes the charge pump performance because output resistance of the charge pump is several dozen kΩ and it matches to a 50 kΩ load. In actual sensor nodes, the charge pump is connected to the storage capacitor and the load impedance is lower than 470 kΩ due to the shunt impedance of the storage capacitor. As we can see, the original impedance of the charge pump is not matched to 50 Ω. Therefore, it is necessary to insert a matching circuit as shown in Figure 6. which consists of 8.2 nH and 10 nH high-frequency inductors welded on the surface of the charge pump circuit board, enabling a sufficient matching in the TV signal bandwidth as shown in Figure 10. In this bandwidth, the S11 values are lower than -6.85 dB when a 50 kΩ load is connected and is lower than -3.64 dB when a 470 kΩ load is connected.

### C. Energy Storage and Sensor Node

The rectified energy is stored in the energy storage, that is, the capacitor in our system. The sensor node wakes up from the sleep mode and senses and transmits the data to the access point. The energy consumption during the process $W_C$ is approcimately 200 $\mu$J for a sensing task including wake-up and sensing operation, and it only consumes several microwatts in the sleep mode. After the sensor node completes the sensing operation, the capacitor voltage must be maintained over $V_{min}$ of 1.8 V. Otherwise, the sensor node turns off because of energy shortage and the sensor node requires 1.03 mJ for initialization, which is five times greater than the power required for a sensing action. Sufficient voltage is necessary to prevent the sensor node in reverting to the "off" mode. The required condition for the capacitor voltage $V_C$ before a sensing task begins is represented as $\frac{C}{2}(V_C^2 - V_{min}^2) \geq W_C$, with capacitance $C$. As a result, the requirement for capacitor voltage $V_C$ is

$$V_C \geq \sqrt{\frac{2W_C}{C} + V_{min}^2} \tag{2}$$

It means that $V_C$ can maintain a value over $V_min$ after the sensing operation is finished, if the $V_C$ is larger than the threshold voltage before the sensing. For example, when a 47-$\mu$F capacitor is selected, $V_C$ should be greater than 3.5 V. When we use a 100-$\mu$F, $V_C$ should be greater than 2.7V, and when a 200-$\mu$F is used, $V_C$ should be greater than 2.3V. Considering a charge pump output voltage close to 3V upon simulation, it is difficult to increase this voltage above 3.5 V. Thus, a capacitance with a value larger than 100 $\mu$F is required as also verified by Nishimoto and Vyas [11], [13]. In addition, a larger capacitance contributes to the suppression of the voltage ripple. The DC leakage of the capacitor is denoted as $kCV_C$ ($k$ is a constant of leakage). A very large capacitance value yields a greater leakage loss. As described on Section III, although the total channel power level dynamically changes when the total channel power state shifts from State A to State B or from State B to State A, the fluctuation range of the harvested energy stay within a dozen $\mu$W except such state changes. It allows the sensor to operate with a low energy buffer. Considering these aspects, we select the capacity of energy storage as 100 $\mu$F.

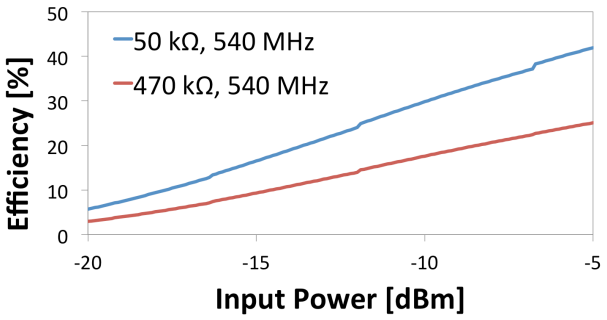


Fig. 11. Performance of charge pump: RF/DC conversion efficiency.

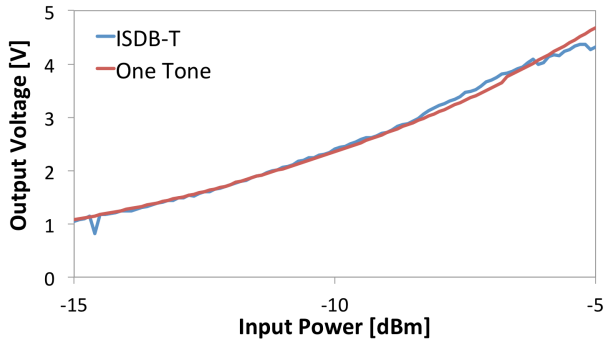


Fig. 12. Performance of charge pump: single-tone vs. ISDB-T TV signal.

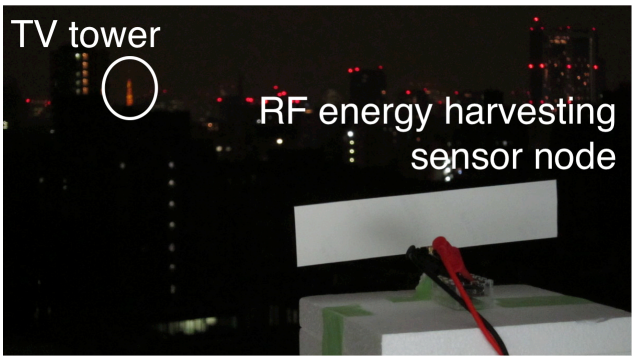


Fig. 13. Experiment with RF energy harvesting sensor node.

## V. Evaluation of Sensor Node

Without loss of generality and for proof of concept verification purposes, we implement a sensor node including an antenna and a charge pump, the design which is discussed in Section IV, and evaluate its performance. First, we measured the RF/DC conversion efficiency of our charge pump and connected the charge pump to a vector signal generator that generates a multi-carrier signal in order to simulate the ISDB-T and confirm the performance of the charge pump when the input signal is not a single-tone signal. Further, we evaluated the activation/performance of the sensor in realistic deployment conditions, that is, on 11th floor of our building that is 6.3 km far away the Tokyo tower.

### A. Performance of Charge Pump

We connected the charge pump to a signal generator, supplying a 540 MHz single-tone signal whose power values swept from -20 dBm to -5 dBm in order to measure the RF/DC conversion efficiency. RF/DC conversion efficiency $\eta$ which is given by the following formula.

$$\eta = \frac{P_{DC}}{P_{RF}} \tag{3}$$

Note that $P_{DC}$ is the output DC power that is supplied to the load and $P_{RF}$ is the input RF power. Figure 11 shows the efficiency values for our benchmarking sensor configuration. When the input level is -10 dBm, the efficiency is 10.0% with 470 kΩ load and 30.0% with 50 kΩ. In this measurement, we utilize a single-tone signal instead of a ISDB-T signal to simplify the testing environment while the input level is estimated to be around -10 dBm using aforementioned Equation 1 [13]. Thus, the measurement result would be slightly different from the actual performance of charge pump because of the effects of multi-career signal. As described in Section III, the Japanese digital TV broadcasting uses the ISDB-T standard and OFDM modulation. Thirteen segments are used to construct a channel of ISDB-T signal. One segment is allocated for mobile TV broadcast and the remaining twelve segments are for high-definition TV broadcast. The bandwidth of each segment is 429kHz, and a 430-kHz guard band is additionally used, thereby the total bandwidth of a channel is 6MHz. A segment can be divided to 432 carriers that are QAM -modulated. Thus, the total number of carriers for a ISDB-T channel is 5617. The ISDB-T signal was simulated by using a Rohde & Schwarz SMBV100A vector signal generator with an arbitrary-waveform baseband signal generator. A unique characteristic of the signal is that its peak envelope power is higher than the average power. This peak can be observed only for a short period, and therefore, the typical sampling rate of the spectrum analyzer is not sufficient to observe the peak; however, it affects the charge pump performance. Figure 12 shows the comparison between the case where the input signal of the charge pump is a single-tone signal (540 MHz) and the case where it is a simulated ISDB-T signal. With the simulated signal, the charge pump performance is better than that obtained with a single-tone signal. When a chaotic spectrum signal is inputted into the rectifier, its output DC voltage and RF-to-DC conversion efficiency are improved [24], an effect that explains the performance improvement when an ISDB-T signal is inserted as verified by Vyas, Kawahara and Tentzeris [13].

### B. Performance in Actual Situation

We placed the sensor node on the balcony of our building from where we could observe the Tokyo tower line of sight (Figure 13). We measure the output voltage of the rectenna and confirm the operation of the sensor node. As described in Section III, the channel power tends to be unstable at daytime and stable at nighttime. This is mainly caused by the different types of fading including k-type fading and duct-type fading due to refractive-index change owing to air temperature

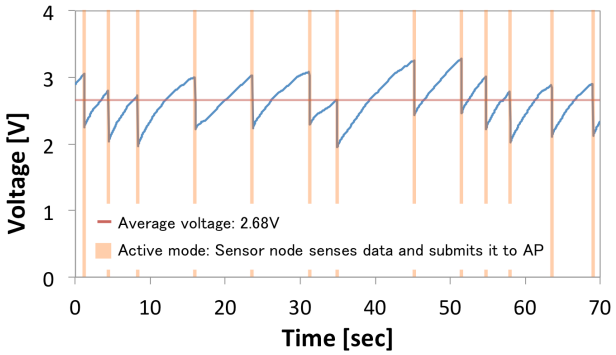


Fig. 14. Capacitor voltage when sensor node periodically wakes up.

change at daytime [25]. We performed the measurement from 11 p.m. to 12 p.m. in order to eliminate the effect of fading. First, we monitored the output voltage when the capacitor is not connected to the sensor node. The capacitor voltage is saturated at approximately 3.8 V; however the output voltage estimated from charging process of the storage capacitor is slightly different. The transition shows that the charge pump operates as 4.1 V equivalent DC voltage source with an output impedance of 100 kΩ. The characteristic of the equivalent DC source (e.g. output voltage) strongly depends on the supplied power. However, the equivalent power source is valuable for the design of a DC circuit including a microcontroller.

### C. Performance of Sensor Node

Figure 14 shows the capacitor voltage when the rectenna, which is placed in the same setup of the previous experiment, is connected to the sensor node, which periodically wakes up and senses the temperature and transmits the sensed data to the access point. The wake-up timing of the sensor node is determined by using the simple duty cycle control method to get robustness of the energy harvester to short-term variability. The duty cycle control method sets the duty cycle to minimize the objective function $f(B_t) = (B^* - B_t)^2$. In this formula, $B_t$ denotes the current stored energy level and $B^*$ denotes the desired stored energy level. The stored energy level is calculated as $\frac{V_C^2}{V_{max}^2}$ using the current capacitor voltage $V_C$ and maximum voltage $V_{max}$. The duty cycle $u_{t+1}$ is set as $u_{t+1} = u_t - a(B^* - B_t)$ ($a$ is a constant used for adjustment sensitivity). In this case, we set the desired voltage to 2.8 V, which implies that $B^* = 0.6$ when $V_{max}$ is 3.6 V, which is a limitation of the DC supply level for the sensor node. We calculated the average voltage during the 70 seconds that are enough long to observe the periodical sensing operation and enough short to avoid effects of TV channel fluctuations. As a result, the average voltage is 2.68V, which is slightly lower than the desired level because the sensor node can sense the capacitor voltage only in the "active" (ON) mode. The duty cycle control method obtains only two parameters: current voltage and current duty cycle. It does not consider the level of the harvested energy, thus it is too sensitive to the harvested energy variability. To make matters worse, the voltage is not convergent under the naive duty cycle control and swinging over the desired voltage, similar to the one shown in Figure 14. Sometimes such unstable control sets the duty cycle too high and the sensor node consumes the stored energy too quickly, consequently switching to the off-mode and requiring significant energy to restart from off-mode to active-mode, thereby reducing drastically its energy efficiency. This duty cycle determination approach is far from optimal control necessitating the development of the much more effective approach introduced in this paper. Although Nishimoto and Vyas have proposed numerous duty cycle determination methods [11], [13], they have not focused on the variability of harvested energy in midnight and leakage characteristics of an energy storage. Our proposed method is focusing on these two factors that commonly prevent the efficient operation of ambient RF energy harvesting sensor node.

## VI. Leakage-Aware Duty Cycle Control

Most microprocessors used for WSNs can reduce the current consumption by entering the sleep state. The transition time between the active mode and the sleep mode is rather short. The energy management software for WSNs is typically realized by using the abovementioned feature, and the objective of the energy management is to determine the duty cycle, that is, the ratio of the duration of the active state to the total period of a repetitive cycle. Kansal et al. introduced the energy neutral operation (ENO) concept [26]. In ENO, the duty cycle is always determined to maintain the condition that the consumed energy is always less than the harvested energy. The ENO concept achieves $B_t > B_0$ for $\forall t > 0$, with an initial stored energy level of $B_0$ and a current stored energy level of $B_t$. ENO is required for system sustainability. By extending the ENO concept, Vigorito et al. proposed ENO-MAX [27]. The objective of this operation is to sustain the condition of $B_t = B_0$ for $\forall t > 0$ because if the harvested energy overshoots the energy consumption, the system does not efficiently use the available energy. Therefore, these researchers defined an objective function as the average of $(B_t - B_0)^2$ for $\forall t > 0$ and applied a control method for minimizing it by using the linear quadratic (LQ) tracking control [28]. In short, this control method enables the system to sustain stored energy level $B_t$ as $B_0$ even if the energy supply is unstable. Thus, $B_0$ is a significantly important parameter of this control method and is considered as the optimal stored energy level.

In the LQ tracking control system, the system operation point is represented by the stored energy level. For an efficient operation, the operation point should track the optimal point, that is, the operation should be performed at the optimal stored energy level. In this study, we propose a calculation method for the optimal stored energy level and a tracking method to enable the operation point to keep the optimal point. By applying the LQ tracking control to the energy harvesting systems, along with the adaptive duty cycle control, an efficient energy management under unstable harvested energy supplies is achieved. However, this method does not obtain the optimal stored energy level. If the energy storage device is a battery, energy loss from energy storage does not depend on its stored energy

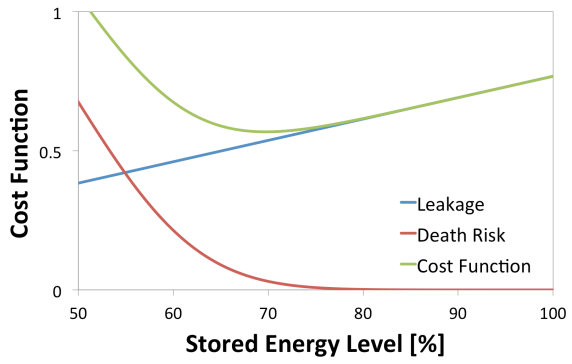


Fig. 15. Aggregate cost function to calculate optimal stored energy level.

level, thus the optimal stored energy level is not crucial for energy efficiency. Therefore, Vigorito et al. have heuristically determined the optimal stored energy level [27]. However, when the energy storage device is a capacitor, the energy loss caused by the leakage is related with its stored level. In this case, the optimal stored energy level determination method is required for energy efficient operations. The objective of our previous study was to calculate and track the operation point; however, it still contained a heuristic parameter [14].

### A. Leakage Aware Optimal Operation Point Calculation

In this section, we demonstrate the optimal stored energy level calculation, considering both capacitor leakage and energy shortage risk. The parameters of this method depend on the specific sensor node designs, such as the characteristics of the energy storage configurations and harvested energy fluctuation patterns that can be estimated by measurements. First, we discuss the capacitor leakage. The capacitor leakage current can be calculated as to be $kCV_C(k \sim 0.01)$ with capacitor voltage $V_C$ and capacitance $C$. The constant value of $k$ is dependent on the type of capacitor and 0.01 is typical value for chemical capacitor. The capacitor leakage energy is denoted as $P_l = kCV_C^2$. Further, the leakage power is proportional to stored energy level $B_t$, which is $\frac{V_C^2}{V_{max}^2}$($V_{max}$ is the maximum capacitor voltage) and is expressed as $P_l = kCV_{max}^2 B_t$. Finally, in $T$ seconds, the normalized leakage energy is given by

$$f_{leak}(B_t) = W_l = k_l B_t T (k_l = kCV_{max}^2) \tag{4}$$

Note that all the energy values, in this section, are normalized by the maximum stored energy in the capacitor $\frac{1}{2}CV_{max}^2$. Second, we attempt to evaluate the energy shortage risk and the loss when the sensor node is dead and forced to restart. Although a microprocessor consumes only several microamperes while in the sleep state, its input voltage is almost always greater than a specific value of 1.8 V. When the input voltage decreases below the specific value, the microprocessor is forced to enter the off state. Thus, we define the minimum stored energy level for the sensor node operation as $B_{min}$. The energy for restarting the sensor node is denoted as $W_r$, the harvested energy is denoted as $W_h$ and the energy used for sensing is denoted as $W_c$ in $T$ seconds. Under this condition, stored energy $B_t$ after $T$ seconds is $B_{t+T} = B_t + W_h - W_c - W_l$. The condition of $B_{t+T} > B_{min}$ is required to continue the sensor node operation. Thus, when $W_h \leq W_c + W_l - (B_t - B_{min})$, the sensor node becomes dead node, the probability of which is expressed with the following probability distribution function:

$$P_{dead}(B_t) = \int_0^{W_c+W_l-(B_t-B_{min})} p(W_h) dW_h \tag{5}$$

By applying the LQ tracking, the relationship between the stored level in next wake-up time and the system parameters including the duty cycle, previous stored energy level, and the optimal stored energy level, is estimated and adjusted to the current system condition including the amount of harvested energy. With the appropriately estimated relationship of these parameters, $W_c + W_l$ is controlled to be close to the average of the harvested energy $E[W_h]$. Therefore, this probability can be approximated by

$$P_{dead}(B_t) = P(E[W_h] - (B_t - B_{min})) \tag{6}$$

using the cumulative distribution function (CDF) $P(W_h)$ of the harvested energy. This implies that the variability in the harvested energy is a significant parameter for eliminating the risk of the sensor to become a dead node. The CDF can be estimated from the harvested energy data like the TV channel power histogram (Figure 4). According to the histogram, the TV channel power fluctuation can be simulated by the normal distribution. Note that the standard deviation represents the level fluctuation of the harvested energy when the CDF is based on the normal distribution. Finally, the energy loss during the sensor node restart due to energy shortage is expressed as

$$f_{dead}(B_t) = P_{dead}(B_t) W_r \tag{7}$$

We determine the aggregate of the losses by summing the above two terms and define the sum as a cost function $f(B_t)$.

$$f(B_t) = f_{leak}(B_t) + f_{dead}(B_t) \tag{8}$$

The aggregated cost function is shown in Figure 15. A stored energy level that minimizes the cost function is the optimal level.

### B. Linear Quadratic Tracking

An optimal control method is applied to the LQ tracking problem. In this case, we consider a linear dynamical system with colored noise. This system is expressed by the formula

$$B_{t+1} = aB_t + bu_t + cw_t + w_{t+1} \tag{9}$$

where $B_t$ is the current stored energy level; $u_t$ is the duty cycle; $w_t$ is the noise; and $a, b$, and $c$ are the real-valued coefficients. When $B^*$ represents the desired stored energy level, the duty cycles should be set to a value obtained as

$$u_t = \frac{B^* - (a+c)B_t + cB^*}{b} \tag{10}$$

for the optimal power control and it does not depend on $w_t$, but does depend on coefficient $c$ of previous noise terms [27].

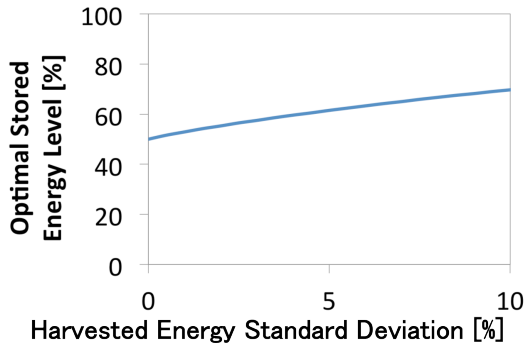


Fig. 16. Relationship between the harvested energy variation and the optimal stored energy level.

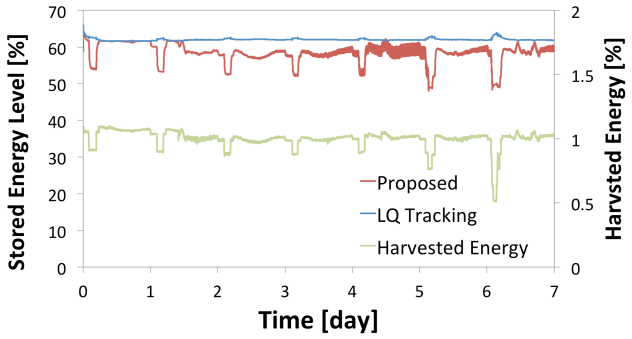


Fig. 17. Simulation result: stored energy level for a week.

In typical situations, $a, b$, and $c$ are initially unknown and can be estimated using a stochastic gradient descent method, with which we determine the duty cycle $u_t$. Further, we define a parameter vector $\theta = (a + c, b, c)^T$ and a feature vector $\phi_t = (B_t, u_t, -B^*)^T$. The estimated vector $\hat{\theta}_{t+1}$ is expressed as

$$\hat{\theta}_{t+1} = \hat{\theta}_t + \frac{\mu}{r_t}\phi_t(B_{t+1} - \phi_t^T\hat{\phi}_t) \tag{11}$$

Where $\mu$ is the a step size and $r_t = \sum_{k=1}^{t}\phi_k^T\phi_k$. Using $\hat{\theta}_{t+1}$, $u_{t+1}$ can be calculated by the aforementioned formula. The step size does not significantly affect to the performance so it should be set to reasonable value as Vigorito et al. reported in [27]. The duty cycle update interval should be short enough to adapt to the harvested energy fluctuations. In our case, the duty cycle should be updated every few minutes to get robustness to TV signal fluctuations.

### C. Optimal Level Adaptation with State Awareness

As mentioned above, the aggregated cost function depends on the level fluctuation of the harvest energy. Thus, when the state of energy supply changes and the level of harvested energy fluctuates, the optimal stored energy level should be recalculated. However, a simple LQ tracking uses the static optimal stored level and therefore, sometimes, leads to inefficient condition of system in some states. Taking the lack of state awareness under consideration, we propose an optimal level adaptation method considering the possible level fluctuation of harvested energy, using standard deviations. We calculate the aggregated cost function and find the minimum point of the cost function for each standard deviation, acquiring a relationship between the standard deviations of harvested energy and the optimal level as shown in Figure 16. In this example, when the fluctuation of harvested energy is sufficiently small, the optimal stored energy level is around 50% that means the sensor node should keep storing 50 % energy of the maximum energy capacity in an energy storage device that is restricted by the maximum operating voltage of a sensor node. On the other hand, when the harvested energy fluctuation is large (above 10%), the optimal stored energy level is around 70 % that means sensor node should keep storing more energy in order to avoid the energy shortage that occurs accidentally caused by the large variabilities of harvester energy. We need to appropriately select an optimal level, considering the harvested energy level fluctuation and aforementioned relations. Furthermore, we attempt to maintain the sensor node operation at the optimal point by the LQ tracking. This proposed method can adjust the optimal level of each state estimated by the level of the harvested energy. When the harvested energy decreases over 10 %, the system considers this event as a state transition and modifies its optimal stored energy level profile. This scheme enables the stored energy level to be set to the optimal level always. As well, the optimal level adaption achieves a significant capacitor leakage reduction.

## VII. Evaluation of Duty Cycle Control

By observing the stored energy level as shown in Figure 17, we can observe that the level was adjusted to be optimal level. The capacitor leakage is proportional to the stored energy level. Thus, the sensor node operation at lower energy level is desirable for leakage reduction. However, the sensor node operation at a very low energy level can cause an energy shortage and consume a large amount of energy to restart the operation. This implies that balancing is quite important for efficient and stable operations. As demonstrated by the simulation results, the proposed method achieves an appropriate balance that can reduce the capacitor leakage without affecting the sustainable operation. We performed the control simulation for a week to evaluate the long-term operation efficiency. As summarized in Table I, the simple LQ tracking uses 73.2% of the supplied energy for sensing operations and loses 26.8% of the energy through leakage. By contrast, the proposed method uses 74.6% of its energy for sensing and loses 25.4% through leakage. This implies that the proposed method achieves a 5.34% leakage reduction. The state awareness enables the system to efficiently use the energy for sensing, thereby reducing the leakage loss. As a result, this method achieves an improvement in the sensing reliability and accuracy by maximizing the sampling rate of the sensing operation.

## VIII. Conclusion

We have introduced a method that realizes an optimal stored energy level calculation and an adaptive duty cycle control using LQ tracking to sustain the optimal stored energy level under the condition of unstable and fluctuating harvested

TABLE I
SIMULATION RESULT: TOTAL AMOUNT OF ENERGY USED IN SIMULATION.

| Method | LQ Tracking | Proposed |
|---|---|---|
| Sensing | 73.2% | 74.6% |
| Leakage | 26.8% | 25.4% |

energy. The proposed method defines and minimizes the cost function by aggregation of the capacitor leakage characteristics and of the energy shortage risk to calculate the optimal level. In addition, the proposed method focuses on both long-term and short-term harvested energy transitions, which are specific characteristics of RF energy harvesting, especially for TV signals. This method monitors the harvested energy and adjusts its optimal stored energy level when long-term changes are detected. This environmental awareness enables an efficient energy usage by capacitor leakage reduction. For a benchmarking sensing topology, the proposed method achieved a 5.34% leakage reduction as compared to simple LQ tracking.

## ACKNOWLEDGMENT

This research was supported in part by the Industrial Technology Research Grant Program, 2009, of the New Energy and Industrial Technology Development Organization (NEDO) of Japan and in part by the U.S. National Science Foundation (NSF).

## REFERENCES

[1] S. Sudevalayam and P. Kulkarni, "Energy harvesting sensor nodes: Survey and implications," *IEEE Communications Surveys Tutorials*, vol. 13, no. 3, pp. 443 –461, July 2011.

[2] C. Moser, L. Thiele, D. Brunelli, and L. Benini, "Adaptive power management in energy harvesting systems," in *the conference on Design, automation and test in Europe*, ser. DATE '07, Nice, France, May 2007, pp. 773–778.

[3] G. Ottman, H. Hofmann, A. Bhatt, and G. Lesieutre, "Adaptive piezoelectric energy harvesting circuit for wireless remote power supply," *Power Electronics, IEEE Transactions on*, vol. 17, no. 5, pp. 669 – 676, sep 2002.

[4] J. Taneja, J. Jeong, and D. Culler, "Design, modeling, and capacity planning for micro-solar power sensor networks," in *the 7th international conference on Information processing in sensor networks*, ser. IPSN '08, St Louis, MI, April 2008, pp. 407–418.

[5] A. Parks, A. Sample, Y. Zhao, and J. R. Smith, "A wireless sensing platform utilizing ambient rf energy," in *IEEE Topical Meeting on Wireless Sensors and Sensor Networks (WiSNET)*, Austin, TX, Jan 2013, pp. 1 –3.

[6] A. Dolgov, R. Zane, and Z. Popovic, "Power management system for online low power rf energy harvesting optimization," *IEEE Transactions on Circuits and Systems I: Regular Papers*, vol. 57, no. 7, pp. 1802 – 1811, July 2010.

[7] T. Le, K. Mayaram, and T. Fiez, "Efficient far-field radio frequency energy harvesting for passively powered sensor networks," *Solid-State Circuits, IEEE Journal of*, vol. 43, no. 5, pp. 1287 –1302, May 2008.

[8] U. Olgun, C.-C. Chen, and J. Volakis, "Design of an efficient ambient wifi energy harvesting system," *IET Microwaves, Antennas Propagation*, vol. 6, no. 11, pp. 1200 –1206, Aug 2012.

[9] G. Andia Vera, A. Georgiadis, A. Collado, and S. Via, "Design of a 2.45 ghz rectenna for electromagnetic (em) energy scavenging," in *Radio and Wireless Symposium (RWS), 2010 IEEE*, New Orleans, LA, Jan. 2010, pp. 61 –64.

[10] M. Roberg, E. Falkenstein, and Z. Popovic, "High-efficiency harmonically-terminated rectifier for wireless powering applications," in *Microwave Symposium Digest (MTT), 2012 IEEE MTT-S International*, Montreal, Canada, June 2012, pp. 1 –3.

[11] H. Nishimoto, Y. Kawahara, and T. Asami, "Prototype implementation of wireless sensor network using tv broadcast rf energy harvesting," in *12th ACM international conference adjunct papers on Ubiquitous computing - Adjunct*, ser. Ubicomp '10 Adjunct, Copenhagen, Denmark, Sep 2010, pp. 373–374.

[12] R. Vyas, H. Nishimoto, M. Tentzeris, Y. Kawahara, and T. Asami, "A battery-less, energy harvesting device for long range scavenging of wireless power from terrestrial tv broadcasts," in *IEEE MTT-S International Microwave Symposium Digest (MTT) 2012*, Montreal, Canada, June 2012, pp. 1 –3.

[13] R. Vyas, B. Cook, Y. Kawahara, and M. Tentzeris, "E-wehp: A battery-less, embedded, sensor-platform wirelessly powered from ambient, digital-tv signals," *IEEE Transactions on Microwave Theory and Techniques*, pp. 1–8, March 2013.

[14] R. Shigeta, Y. Kawahara, and T. Asami, "Demo: Capacitor leakage aware duty cycle control for energy harvesting wireless sensor networks," in *9th ACM Conference on Embedded Networked Sensor Systems*, ser. SenSys '11, Seattle, WA, Nov 2011, pp. 387–388.

[15] Yagi Antenna.Inc, "UwPA: UHF antenna," http://www.yagi-antenna.co.jp/global/products/home.html, 2005.

[16] D. Willkomm, S. Machiraju, J. Bolot, and A. Wolisz, "Primary users in cellular networks: A large-scale measurement study," in *3rd IEEE Symposium on New Frontiers in Dynamic Spectrum Access Networks (DySPAN) 2008*, Chicago, IL, Oct 2008, pp. 1 –11.

[17] Texas Instruments, "eZ430-RF2500," http://www.ti.com/tool/ez430-rf2500, 2009.

[18] T. Yoshiaki, S. Shino, and K. Kobasyashi, "Process for preparing conductive material," Patent US 8 013 676B2, Sep. 6, 2011.

[19] F. Yuan and N. Soltani, "Design techniques for power harvesting of passive wireless microsensors," in *51st Midwest Symposium on Circuits and Systems (MWSCAS) 2008*, Aug 2008, pp. 289 –293.

[20] Seiko Instruments Inc., "Ultra-low voltage operation charge pump IC for step-up DC-DC converter startup S-882Z series," http://datasheet.sii-ic.com/en/charge_pump_ic/S882Z_E.pdf, 2010.

[21] Skyworks Solutions, Inc., "Surface mount mixer and detector Schottky diodes," http://www.skyworksinc.com/uploads/documents/200041V.pdf, 2012.

[22] K. Lui, A. Vilches, and C. Toumazou, "Ultra-efficient microwave harvesting system for battery-less micropower microcontroller platform," *IET Microwaves, Antennas Propagation*, vol. 5, no. 7, pp. 811 –817, May 2011.

[23] Avago Technologies, "HSMS-286x surface mount RF Schottky barrier diodes," http://www.avagotech.com/docs/AV02-1388EN, 2009.

[24] A. Collado and A. Georgiadis, "Improving wireless power transmission efficiency using chaotic waveforms," in *IEEE MTT-S International Microwave Symposium Digest (MTT) 2012*, Montreal, Canada, June 2012, pp. 1 –3.

[25] G. W. Collins, *Fundamentals of digital television transmission*. Wiley, 2001.

[26] A. Kansal, J. Hsu, S. Zahedi, and M. B. Srivastava, "Power management in energy harvesting sensor networks," *ACM Trans. Embed. Comput. Syst.*, vol. 6, no. 4, Sep 2007.

[27] C. Vigorito, D. Ganesan, and A. Barto, "Adaptive control of duty cycling in energy-harvesting wireless sensor networks," in *4th Annual IEEE Communications Society Conference on Sensor, Mesh and Ad Hoc Communications and Networks (SECON) 2007*, June 2007, pp. 21 –30.

[28] P. R. Kumar and P. Varaiya, *Stochastic systems: estimation, identification and adaptive control*. Upper Saddle River, NJ: Prentice-Hall, Inc., 1986.